CMS Physics Analysis Summary

Contact: cms-pog-conveners-lum@cern.ch 2021/04/29

Luminosity measurement in proton-proton collisions at 5.02 TeV in 2017 at CMS

The CMS Collaboration

Abstract

The measurement of the integrated luminosity for the proton-proton collisions run at a center-of-mass energy of 5.02 TeV in 2017 with the CMS experiment is reported. The absolute luminosity scale is calibrated with the van der Meer scan method. The precision of the calibration is limited by the estimation of the beam separation, the description of electromagnetic interactions between colliding proton bunches, and the uncertainty in the estimated factorization bias. Continuous rate measurements with the forward hadron calorimeter and the Pixel Luminosity Telescope provide a very stable and linear luminosity measurement. The integrated luminosity recorded by the CMS experiment when the detector was fully operational is measured to be $302\,\mathrm{pb}^{-1}$, with a relative uncertainty of 1.9%.

1 Introduction

A well established and precise method to measure the instantaneous luminosity at hadron colliders is based on the van der Meer (vdM) scan technique [1]. The method has been used at all major LHC experiments [2–10]. In vdM scans, the beam axes are moved in the transverse plane across each other such that the "beam overlap integral" can be determined. From the measured overlap integral, and the beam currents, the instantaneous luminosity during the vdM scan is then extracted [11].

To transfer the luminosity information from vdM scans to physics-running conditions at a high number of proton-proton (pp) collisions in a single bunch crossing ("pileup"), rate measurements are performed during the vdM scans with specific luminosity detectors. The absolute scale, i.e., the relation between the rate in a given detector and the luminosity, is a detector-specific constant, usually referred to as the visible cross section σ_{vis}. It relates the rate $\mathrm{d}N/\mathrm{d}t$ to the instantaneous luminosity through the relation $\mathrm{d}N/\mathrm{d}t = \mathcal{L}\sigma_{\text{vis}}$. This aspect of the analysis is described in Section 2.

The integrated rate measurement, performed throughout the entire data-taking period and normalized to σ_{vis}, corresponds to the integrated luminosity. Possible dependencies of the measured rate on the instantaneous or integrated luminosity, such as out-of-time pileup or aging, are continuously monitored using several luminosity detectors, as presented in Section 3.

In this note, we report the measurement of the integrated luminosity at the CMS experiment for the data-taking period in Nov 2017 when the LHC was operated with pp collisions at a center-of-mass energy of 5.02 TeV.

The CMS detector is a multipurpose apparatus designed to study high-p_{T} physics processes in pp collisions, as well as a broad range of phenomena in nuclear collisions. Details are described in Ref. [12]. For the analysis presented here, information from the forward hadron (HF) calorimeter with the occupancy-based method (HFOC) and from the silicon pixel detector with the pixel cluster counting method (PCC) are used, as well as measurements from two dedicated luminosity detectors: the Pixel Luminosity Telescope (PLT) [13], and the silicon sensor of the Fast Beam Condition Monitor (BCM1F) [14]. For details on the various luminosity detectors, we refer to Ref. [3, 4].

2 Analysis of the van der Meer scan data

A vdM scan program was performed during LHC fill 6380 on 11 Nov 2017, with 22 bunch pairs colliding with a crossing angle of 170 μrad at the CMS interaction point. Six scans were performed: four beam-imaging scans, followed by a vdM scan pair. In the vdM scans, the two beams are separated by $6\sigma_b \approx 400\,\mu$m in either x or y, and scanned across one another in a sequence of 17 steps with a step size of $0.75\,\sigma_b \approx 50\,\mu$m, where σ_b is the transverse bunch size. In the beam-imaging scans, one beam is kept fixed at its nominal head-on position while the other is separated and scanned in 19 steps from $-4.5\,\sigma_b$ to $+4.5\,\sigma_b \approx 300\,\mu$m.

To monitor the beam orbits during vdM scans, two independent beam position monitor (BPM) systems are used: the DOROS BPMs [15] located near the CMS detector, and the BPMs located in the LHC arcs adjacent to CMS (arc BPMs). For the latter, the beam position measurement is transformed to a beam position at the CMS interaction point using LHC optics files provided by the LHC operators [16]. Additionally, the primary-vertex reconstruction with the CMS tracker system [17] is used to monitor the movement of the luminous region. The beam positions during the scan program measured with the DOROS BPMs are shown in Fig. 1.

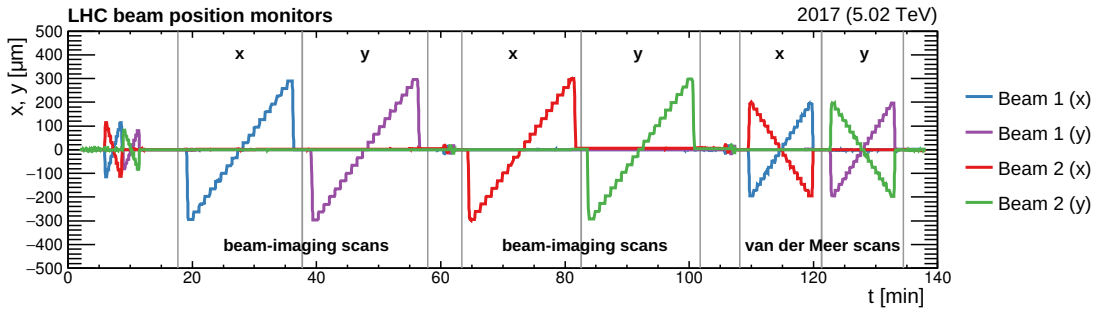

Figure 1: Horizontal and vertical positions of the proton beams measured with the DOROS BPMs during LHC fill 6380. The full vdM data set consists of four beam-imaging scans and one vdM scan pair, delineated by gray vertical lines. The origin of time corresponds to 11 Nov 2017, 07:42 GMT.

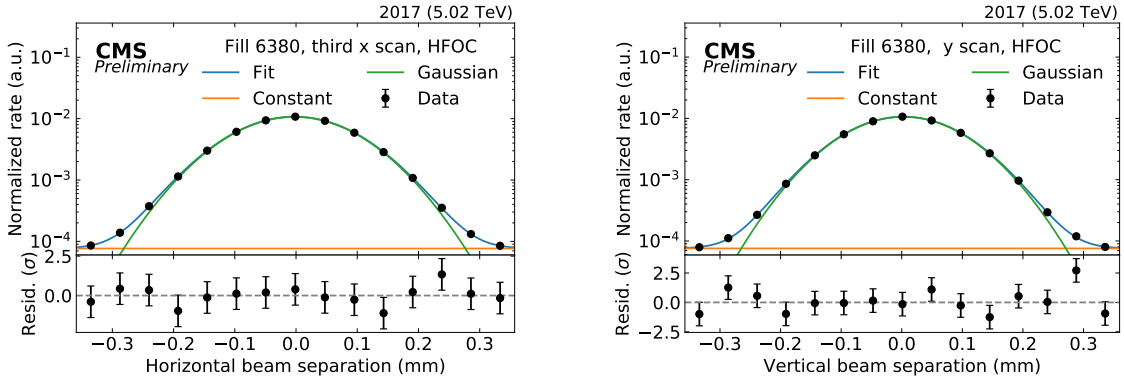

Figure 2: Single-Gaussian plus constant fits to the HFOC data recorded during the third x (left) and y (right) scans. The constant term accounts for background. In the bottom panels, the difference between the measured rate and the fit divided by the statistical uncertainty is shown.

The rate measured in a given detector during a vdM scan is normalized with the measured bunch proton numbers and fitted as a function of the beam separation $\Delta\chi$, $\chi = x, y$, using a single-Gaussian model plus a constant term b_χ to account for background:

$$r_\chi \exp\left(-\frac{(\Delta\chi - \mu_\chi)^2}{\Sigma_\chi^2}\right) + b_\chi. \tag{1}$$

The visible cross section is then measured from an x–y scan pair, using the fit parameters Σ_x, Σ_y, i.e., the "widths" of the single-Gaussian model, as:

$$\sigma_{\text{vis}} = 2\pi\,\Sigma_x\Sigma_y\langle r\rangle, \tag{2}$$

where $\langle r\rangle$ is the average amplitude of the fitted scan curves in x and y. To correctly determine σ_{vis}, a number of corrections are applied that are described in the following. Example fit results are shown in Fig. 2 for HFOC, and in Fig. 3 for PLT.

2.1 Bunch current measurement

The bunch populations are estimated from the bunch currents measured with the Fast Bunch Current Transformers (FBCTs) with a bunch-by-bunch granularity [18]. A more precise measurement of the total beam current with a relative precision of 0.2% is provided by the Direct-Current Current Transformers (DCCTs) [19], and is used to normalize the FBCT measurement,

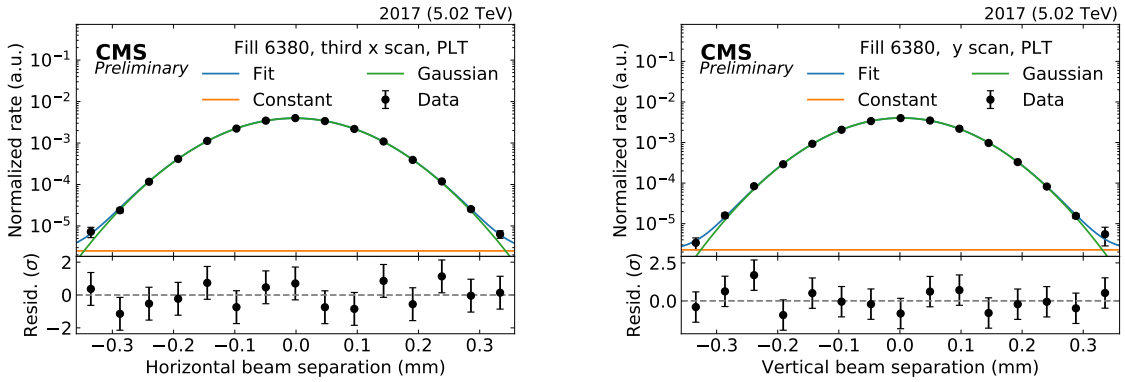

Figure 3: Single-Gaussian plus constant fits to the PLT data recorded during the third x (left) and y (right) scans. The constant term accounts for background. In the bottom panels, the difference between the measured rate and the fit divided by the statistical uncertainty is shown.

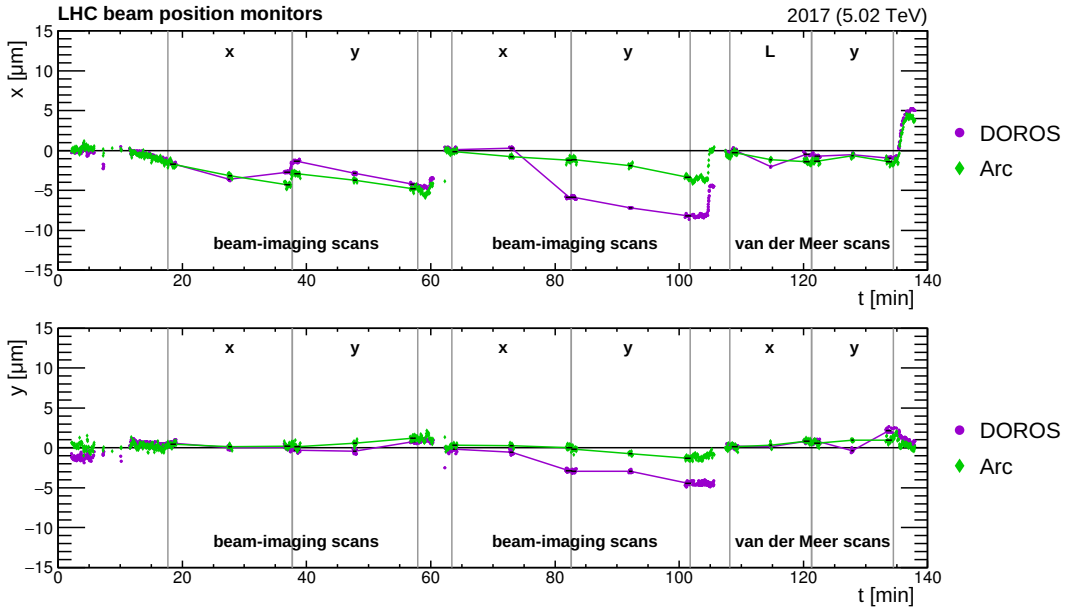

Figure 4: Orbit drift measurements in x (top) and y (bottom) during LHC fill 6380. Points correspond to beam positions measured by the DOROS and arc BPMs in μm at three instances where the beams collide head-on, i.e., before, during (at the head-on step), and after each scan. Lines correspond to linear fits from which the orbit drift at each scan step is estimated. The origin of time corresponds to 11 Nov 2017, 07:42 GMT.

resulting in a correction of 0.6% on σ_{vis}. The presence of noncolliding protons in nominally empty bunches ("ghosts") or out-of-time ("satellites") affects the measurement of the bunch currents and is subtracted [20]. Ghost- and satellite-charge contributions are measured by the Longitudinal Density Monitors (LDMs) and found to be small, resulting in a correction of 0.03% on σ_{vis}. An independent measurement of the ghost charge performed with the beam-gas imaging method at the LHCb experiment [21] shows good agreement with the measurements of the LDMs. The overall uncertainty due to the bunch current measurement is estimated to be 0.2%.

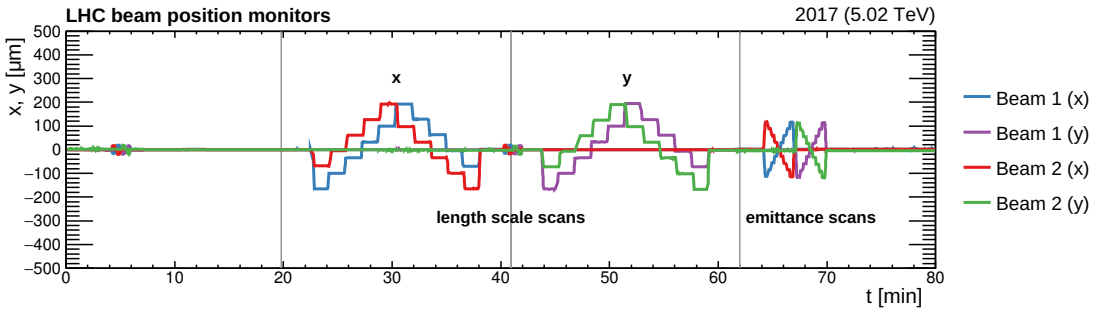

Figure 5: Horizontal and vertical positions of the proton beams measured by the DOROS BPMs during LHC fill 6381, where a length scale scan pair and an emittance scan, a short variant of a vdM scan [22], was performed. The origin of time corresponds to 12 Nov 2017, 10:00 GMT.

2.2 Orbit drift

The term "orbit drift" refers to a possible time-dependency of the transverse beam positions for fixed ("nominal") machine parameters. To determine the beam position movements, the measurements of the DOROS BPMs and arc BPMs are compared. In Fig. 4, the measured positions are shown for three instances in which the beams collide head-on: before, at the head-on step, and after each scan. Linear fits are performed between the measurements before and during the scan to estimate the orbit drift for the first half, and similarly for the second half of the scan. Drifts of up to $\pm 5\,\mu$m are observed. The two monitors are generally in good agreement, except for the time range between about 80 and 100 min where the DOROS BPMs show significant deviations caused by a gain switch. Thus, we use the arc BPMs as the primary measurement and the DOROS BPMs for the uncertainty estimation. Time-dependent position corrections as determined from the arc BPMs are applied to the measurement, resulting in an increase of 0.04% in σ_{vis}. The systematic uncertainty is estimated considering half of the difference between the results using the two different BPMs, and is found to be about 0.3%.

2.3 Length scale calibration

During the beam-imaging and vdM scans, dipole magnets located on both sides of the interaction point are used to separate the beams. The beam positions derived from the LHC magnets are calibrated with information from the CMS tracker, using the average position of the reconstructed vertices as an estimate for the luminous region ("beamspot") position.

In LHC fill 6381, recorded on 12 Nov 2017 with 512 bunch pairs colliding at a crossing angle of 170 μrad in the CMS interaction point, length scale scans were performed. During each scan, the beams are separated by a fixed amount of $1\,\sigma_b \approx 65\,\mu$m in one transverse direction, and then moved coherently forward and backward in five steps in the same transverse direction. In Fig. 5, the measured beam positions of these scans are shown. Primary-vertex reconstruction is used for collision events recorded with a "zero-bias" trigger [23]. The length scale calibration method is described in Ref. [5].

In Fig. 6, the difference between the measured beamspot and nominal positions is plotted against the latter, and fitted with a linear function separately for the forward and backward scan directions. The nominal position is corrected for orbit drift as measured with the DOROS BPMs, following the orbit drift correction procedure described in Ref. [5]. An alternative orbit drift correction derived from arc BPM measurements gives compatible results but with larger deviations from the linear fit. If the LHC magnets produced the nominal positions perfectly, a constant relation, i.e., a linear relation with zero slope, would be observed. The average of the measured slopes from the forward and backward directions is used to determine a correction

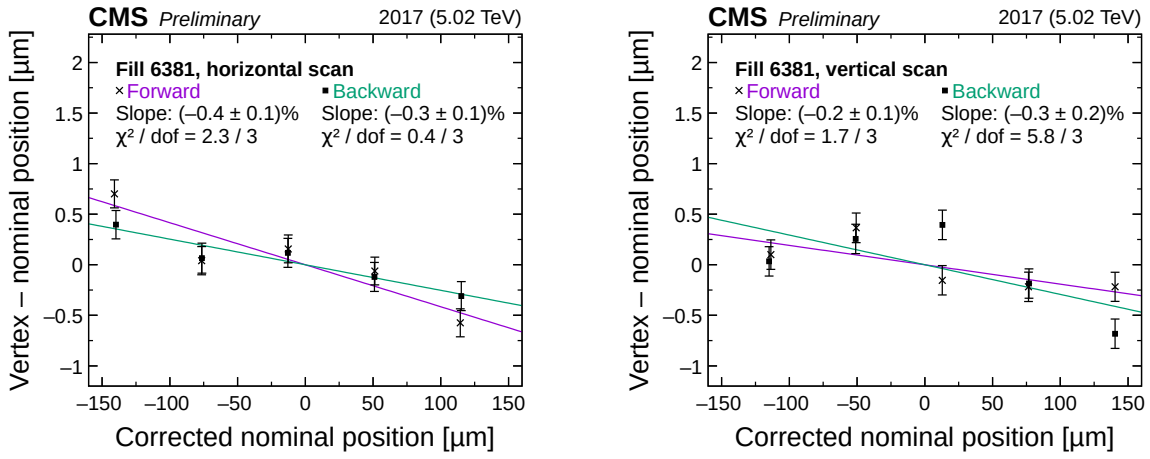

Figure 6: Difference between the reconstructed beamspot and the nominal positions, as a function of the latter, during the length scale scans. The results are shown for the x (left) and y (right) scans, separately for the forward (purple) and backward (green) directions. Nominal positions are corrected for orbit drift. The lines denote linear fits with slope and χ^2/dof values shown in the legend.

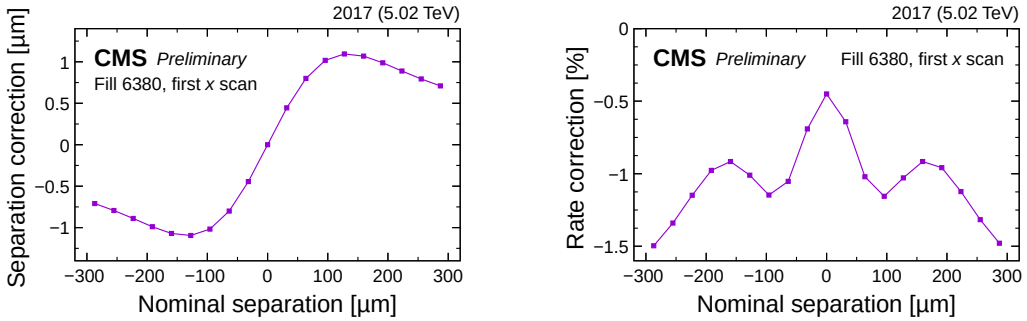

Figure 7: Correction on the beam separation from beam-beam deflection (left), and correction on the rate measurement from the incoherent beam-beam effect (right). The corrections are shown for the first x scan.

to the beam separation in the fits to the vdM scan data.

The resulting corrections are -0.3% in x and -0.2% in y. The average step size measured with the DOROS BPMs, which is used to derive the orbit drift correction, has an uncertainty of 0.7% which is propagated to the uncertainty in the length scale corrections. Other sources of uncertainty include the differences between the forward and backward scans, the statistical uncertainty from the fit, and the possible impact of tracker misalignment, resulting in a total uncertainty of 0.8%.

2.4 Beam-beam effects

Electromagnetic interactions between two colliding proton bunches impact both the transverse separation of the bunches as well as the density distribution of the protons in the bunches. Two beam-beam effects are distinguished: the coherent and the incoherent effect.

Due to their electromagnetic repulsion, an angular kick induces a coherent shift in the closed orbits of the bunches. The increase in the absolute beam separation, also known as "beam-beam deflection", is calculated based on the Bassetti-Erskine formula [24] ignoring the negligible impact of the crossing angle [25]. The resulting correction is shown in Fig. 7 (left). It increases

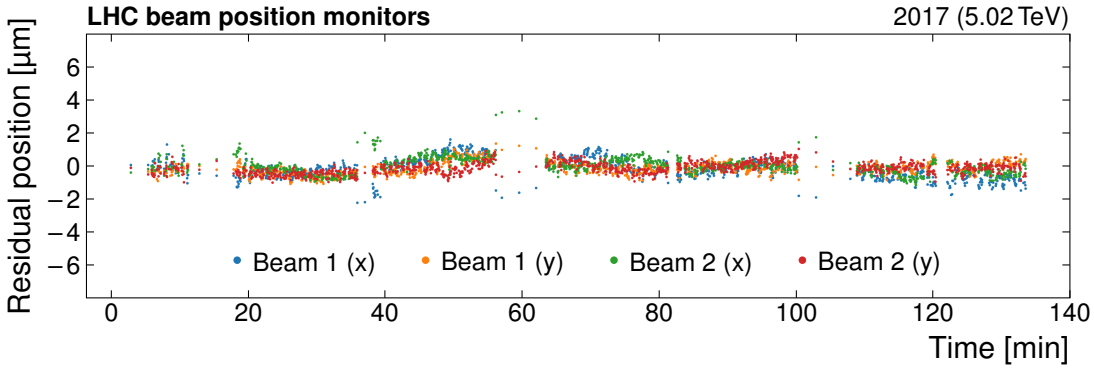

Figure 8: Residual horizontal and vertical positions of the proton beams measured by the arc BPMs during LHC fill 6380, after the orbit drift correction has been subtracted. The origin of time corresponds to 11 Nov 2017, 07:42 GMT.

the Σ_x and Σ_y values, and hence the measured σ_{vis}.

The incoherent effect describes the change of the proton density distributions in the bunches due to the per-particle deflection. It results in a change in the effective β^*, and thus in the measured luminosity. This effect is also known as "dynamic-β" effect. A correction is derived numerically with a dedicated particle tracking program [26, 27], and shown in Fig. 7 (right). Contrary to beam-beam deflection, it decreases the Σ_x and Σ_y values, and hence the measured σ_{vis}.

The combined correction for beam-beam effects results in a small increase of the measured σ_{vis} by 0.4%. The largest source of systematic uncertainty arises from the expected shift in betatron tune values due to simultaneous collisions in the other LHC interaction points, for which we assign an uncertainty of 0.8%.

2.5 Residual beam position differences

In addition to orbit drift, length scale, and beam-beam deflection, the actual beam separation at each scan step can be affected by systematic deviations of the beam positions from their nominal settings, which impact the measured rate at each scan step [5]. In Fig. 8, the beam positions measured with the arc BPMs, which do not include the nominal beam offsets due to the position of the arc BPMs outside the steering magnets, are shown after the orbit drift as estimated in Section 2.2 has been subtracted. The length scale of the arc BPMs, i.e., a small correlation of the measured arc BPM positions with the nominal beam offsets due to imperfect magnet settings, is not included. Beam-beam deflection is visible in the residual beam positions, but the magnitude of the effect in the arc BPM measurement is not well understood. To account for such deviations of the beam positions of up to 2 μm away from the nominal orbit, we assign an uncertainty of 1% in σ_{vis}.

2.6 Factorization bias

The vdM scan method assumes that the transverse proton bunch densities factorize into x- and y-dependent functions. When the transverse proton bunch densities exhibit intrinsic nonfactorization, or when the coordinates of the factorization deviate from the coordinates used for the vdM scans, the measured luminosity is biased.

To estimate the factorization bias, the beam-imaging method [28, 29] is applied. By combining all primary-interaction vertices from one beam-imaging scan, the dependence of the transverse vertex positions on the moving beam's proton bunch density is integrated out in the direction

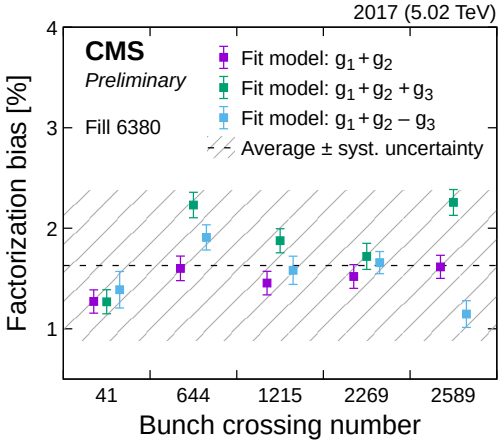

Figure 9: Factorization bias derived from the beam-imaging fit results obtained for different bunch crossings and fit models. The horizontal line denotes the mean value of 1.6%, and the shaded region the uncertainty of 0.8%. The fit models are defined in Ref. [29].

of the scan, hence allowing to extract the x–y correlations present in the resting beam's proton bunch density. From a simultaneous fit to the data of all four beam-imaging scans, the full two-dimensional proton bunch densities are extracted.

In LHC fill 6380, the zero-bias triggers were gated on five colliding bunch pairs, resulting in five data sets which are analyzed independently. For these data sets, good fit results are achieved with normalized sums of two or three single-Gaussian functions as proton bunch density models, where the weight of one of the single-Gaussian functions can be negative. The difference between the measured luminosity from simulated vdM scan data using the fit results as input and the direct integration of the product of the two proton bunch densities yields the factorization bias. These values are shown in Fig. 9, separately for different bunch crossings and different fit models.

The mean value of the factorization bias is found to be 1.6%, and is applied as a correction to the measured σ_{vis}. A systematic uncertainty of 0.8% is assigned to account for the statistical uncertainty of the vdM scan simulation, as well as differences between results obtained for different bunch crossings and fit models.

2.7 Visible cross section results

The visible cross section is measured for HFOC and PLT, including all corrections as previously described. The results obtained separately for the different bunch crossings and x–y scan pairs are summarized in Fig. 10. In general, good agreement among the separate measurements is observed, with slightly larger σ_{vis} values in the vdM scan pair as opposed to the two beam-imaging scan pairs. For HFOC, the σ_{vis} results obtained for some bunch crossings are significantly larger than those for other bunch crossings, coherently for all three x–y scan pairs, which is explained by small differences in capacitor values used in the HF readout circuits. The weighted average of σ_{vis} is 513.0 μb with a statistical uncertainty of 0.02% for HFOC, and 194.1 μb with a statistical uncertainty of 0.06% for PLT.

The consistency between the measured σ_{vis} values is used to estimate the uncertainty due to possible systematic differences between different scan pairs or bunch crossings. The standard deviation of σ_{vis} obtained for the three different scan pairs at the same bunch crossing ("scan-to-scan variation") is on average 0.4% both for HFOC and PLT. Similarly, the "bunch-to-bunch variation" amounts to 0.5% for HFOC and 0.4% for PLT.

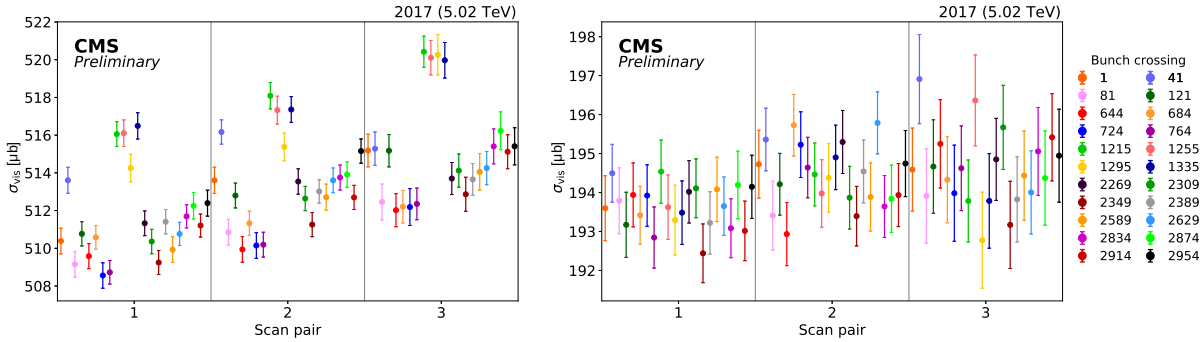

Figure 10: Visible cross section results using the HFOC (left) and PLT (right) measurements, shown chronologically for all x–y scan pairs (where 1 and 2 are the beam-imaging scans), and evaluated for different bunch crossings. All corrections are applied.

While σ_{vis} is a property of the luminosity detector and depends on the detector geometry, acceptance, and efficiency, the width and height of the luminous region in the vdM fill should give the same result for both detectors. Good agreement is observed between the two measurements, and the largest difference in $\Sigma_x\Sigma_y$ of 0.4% is observed for the third x–y scan pair. To describe potential systematic differences between the two detectors, a cross-detector consistency uncertainty of 0.4% is assigned.

3 Transfer to physics-running conditions and integration

The vdM calibration is carried out at low pileup and at an instantaneous luminosity of a few Hz/μb, contrary to the physics-running period characterized by higher pileup. Ideally, the measured rate during physics-running periods is proportional to the instantaneous luminosity, and σ_{vis} is the proportionality constant. In practice, however, corrections for out-of-time (OOT) pileup contributions are applied to the detector response to improve the linearity. The time stability of the detector response as well as residual nonlinearities are evaluated to estimate the systematic uncertainty.

To determine the luminosity recorded by the CMS experiment, an additional uncertainty due to the deadtime of the CMS DAQ system has to be taken into account. It is found to be smaller than 0.1%.

3.1 Out-of-time pileup corrections

Two types of corrections for OOT pileup are considered, following the procedure described in Ref. [3]. "Type-1" corrections account for spill-over from neighboring bunches, while "type-2" effects account for the exponentially decaying afterglow following a colliding bunch due to activation of the surrounding detector material.

For HFOC, residual contributions from OOT pileup are evaluated from the measured rates in nominally empty bunches following filled bunches, using the first empty bunch for the estimation of type-1 residuals, and the second and following empty bunches for type-2 residuals. The type-1 residuals are found to be negligible, with a value of smaller than 0.01% compared to the luminosity of the filled bunch. The distribution of the type-2 residuals as a function of the average single-bunch instantaneous luminosity (SBIL) is shown in Fig. 11. The residuals are smaller than 0.2%, and hence a systematic uncertainty of 0.2% is assigned to the integrated luminosity.

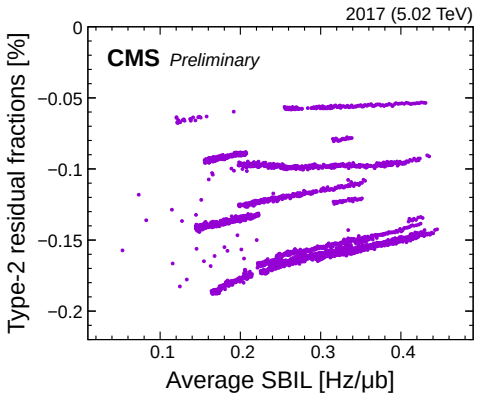

Figure 11: Type-2 residual fractions of the OOT pileup correction to the HFOC response, evaluated as the ratio of the luminosity of the second and following bunches after a colliding bunch to the luminosity of the colliding bunch, after the corrections are applied, for the entire data-taking period at 5.02 TeV in 2017. The fractions are shown as a function of the average single-bunch instantaneous luminosity.

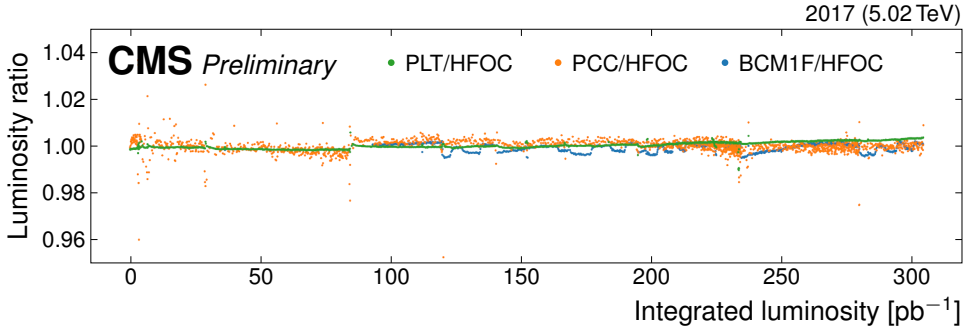

Figure 12: Ratio of the instantaneous luminosity measurement between PLT and HFOC (green), BCM1F and HFOC (blue), and PCC and HFOC (orange) as a function of the integrated luminosity, for the entire data-taking period at 5.02 TeV in 2017.

Effects of the out-of-time pileup for PLT data are assumed to be small and no corrections are applied. The possible background level in the PLT data is estimated from the constant term of the fits to the vdM data, which is assigned as the OOT pileup uncertainty of 0.03%.

3.2 Cross-detector stability

The measurements of the instantaneous luminosity from the different luminosity detectors are compared as a function of time. In Fig. 12, the ratios between the measurements provided by HFOC, PLT, BCM1F, and PCC are shown. The normalization of the HFOC and PLT measurements agree very well over the entire data-taking period. A measurement with the BCM1F silicon sensor is only available for a part of the data-taking period. The absolute luminosity measurements both for PCC and BCM1F are calibrated to the HFOC luminosity measurement. Both measurements confirm the good stability of the detector response. From the width of the distribution of the ratios between the HFOC and PLT luminosity measurement, the cross-detector stability uncertainty is estimated to be 0.14%.

3.3 Cross-detector linearity

To evaluate residual nonlinearities in the detector response, the ratio of the luminosity measurements of different detectors is shown as a function of the instantaneous luminosity in Fig. 13. A

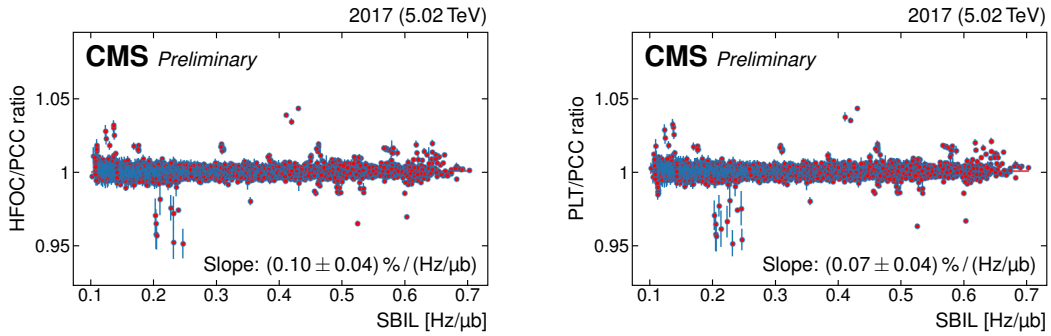

Figure 13: Ratio of the instantaneous luminosity measurement between HFOC and PCC (left), and between PLT and PCC (right) as a function of the single-bunch instantaneous luminosity (SBIL) measured with PCC, for the entire data-taking period at 5.02 TeV in 2017. The slopes and their statistical uncertainties from linear fits to the data are given.

very good linearity is observed both for the HFOC and PLT detector response, each in comparison to the PCC luminosity measurement which is known to be very linear. With a maximum slope of a first-order polynomial fit of 0.1%/(Hz/μb) and an average SBIL of 0.3 Hz/μb for the whole data-taking period at 5.02 TeV in 2017, a cross-detector linearity uncertainty smaller than 0.1% is obtained.

4 Conclusion

Table 1: Summary of contributions to the systematic uncertainty of the integrated luminosity measurement for the proton-proton data-taking period at 5.02 TeV in 2017.

	HFOC	PLT
Calibration uncertainties [%]		
Bunch current measurement	0.2	
Orbit drift	0.3	
Length scale calibration	0.8	
Beam-beam effects	0.8	
Residual beam position differences	1.0	
Factorization bias	0.8	
Statistical uncertainty	<0.1	
Scan-to-scan consistency	0.4	
Bunch-to-bunch consistency	0.5	0.4
Cross-detector consistency	0.4	
Transfer and integration uncertainties [%]		
Out-of-time pileup corrections	0.2	<0.1
Cross-detector stability	0.1	
Cross-detector linearity	<0.1	
CMS deadtime	<0.1	
Total uncertainty [%]	1.9	

The integrated luminosity for the proton-proton data-taking period at a center-of-mass energy of 5.02 TeV in 2017 is measured with the HFOC method and the PLT detector. The absolute

luminosity scale is obtained from the van der Meer method. The integrated luminosity delivered to the CMS experiment is measured to be 341 pb^{-1}. Excluding all periods where the CMS detector was not fully operational, a recorded integrated luminosity of 302 pb^{-1} is estimated. The relative uncertainty of the integrated luminosity measurement is 1.9%, as detailed in Table 1. The dominant contribution to the systematic uncertainty arises from the calibration of the absolute scale of the beam separation, the calculation of electromagnetic interactions between colliding proton bunches, residual beam position differences, and the estimation of the factorization bias.

References

[1] S. van der Meer, "Calibration of the effective beam height in the ISR", ISR Report CERN-ISR-PO-68-31, 1968.

[2] CMS Collaboration, "CMS luminosity calibration for the pp reference run at $\sqrt{s} = 5.02$ TeV", CMS Physics Analysis Summary CMS-PAS-LUM-16-001, 2016.

[3] CMS Collaboration, "CMS luminosity measurement for the 2017 data-taking period at $\sqrt{s} = 13$ TeV", CMS Physics Analysis Summary CMS-PAS-LUM-17-004, 2018.

[4] CMS Collaboration, "CMS luminosity measurement for the 2018 data-taking period at $\sqrt{s} = 13$ TeV", CMS Physics Analysis Summary CMS-PAS-LUM-18-002, 2019.

[5] CMS Collaboration, "Precision luminosity measurement in proton-proton collisions at $\sqrt{s} = 13$ TeV in 2015 and 2016 at CMS", 2021. arXiv:2104.01927. Submitted to *Eur. Phys. J. C*.

[6] ALICE Collaboration, "Measurement of visible cross sections in proton-lead collisions at $\sqrt{s_{\mathrm{NN}}} = 5.02$ TeV in van der Meer scans with the ALICE detector", *JINST* **9** (2014) P11003, doi:10.1088/1748-0221/9/11/P11003, arXiv:1405.1849.

[7] ALICE Collaboration, "ALICE luminosity determination for pp collisions at $\sqrt{s} = 5$ TeV", Technical Report ALICE-PUBLIC-2016-005, 2016.

[8] ALICE Collaboration, "ALICE 2017 luminosity determination for pp collisions at $\sqrt{s} = 5$ TeV", Technical Report ALICE-PUBLIC-2018-014, 2018.

[9] ATLAS Collaboration, "Luminosity determination in pp collisions at $\sqrt{s} = 8$ TeV using the ATLAS detector at the LHC", *Eur. Phys. J. C* **76** (2016) 653, doi:10.1140/epjc/s10052-016-4466-1, arXiv:1608.03953.

[10] LHCb Collaboration, "Precision luminosity measurements at LHCb", *JINST* **9** (2014) P12005, doi:10.1088/1748-0221/9/12/P12005, arXiv:1410.0149.

[11] P. Grafström and W. Kozanecki, "Luminosity determination at proton colliders", *Prog. Part. Nucl. Phys.* **81** (2015) 97, doi:10.1016/j.ppnp.2014.11.002.

[12] CMS Collaboration, "The CMS experiment at the CERN LHC", *JINST* **3** (2008) S08004, doi:10.1088/1748-0221/3/08/S08004.

[13] CMS Collaboration, P. Lujan, "Performance of the Pixel Luminosity Telescope for luminosity measurement at CMS during Run 2", in *Proceedings, 2017 European Physical Society Conference on High Energy Physics (EPS-HEP 2017): Venice, Italy, July 5–12, 2017. PoS* **314** (2017) 504. doi:10.22323/1.314.0504.

[14] CMS Collaboration, M. Guthoff, "The new fast beam condition monitor using poly-crystalline diamond sensors for luminosity measurement at CMS", in *Proceedings, 14th Pisa Meeting on Advanced Detectors: Frontier Detectors for Frontier Physics (Pisameet): La Biodola-Isola d'Elba, Livorno, Italy, May 27–June 2, 2018*. *Nucl. Instrum. Meth. A* **936** (2019) 717. doi:10.1016/j.nima.2018.11.071.

[15] M. Gasior, J. Olexa, and R. Steinhagen, "BPM electronics based on compensated diode detectors—results from development systems", in *Proceedings of the 2012 Beam Instrumentation Workshop (BIW'12)*, p. 44 (MOPG010). 2012.

[16] T. Persson et al., "LHC optics corrections in Run 2", in *Proceedings, 9th Evian Workshop on LHC beam operation*, p. 59. 2019.

[17] CMS Collaboration, "Description and performance of track and primary-vertex reconstruction with the CMS tracker", *JINST* **9** (2014) P10009, doi:10.1088/1748-0221/9/10/P10009, arXiv:1405.6569.

[18] G. Anders et al., "Study of the relative LHC bunch populations for luminosity calibration", Technical Report CERN-ATS-Note-2012-028 PERF, 2012.

[19] C. Barschel et al., "Results of the LHC DCCT calibration studies", Technical Report CERN-ATS-Note-2012-026 PERF, 2012.

[20] A. Alici et al., "Study of the LHC ghost charge and satellite bunches for luminosity calibration.", Technical Report CERN-ATS-Note-2012-029 PERF, 2012.

[21] C. Barschel, "Precision luminosity measurement at LHCb with beam–gas imaging". PhD thesis, RWTH Aachen University, 2014. CERN-THESIS-2013-301.

[22] CMS Collaboration, O. Karacheban, "Long-term monitoring of delivered luminosity and calibration stability in the CMS experiment", in *Proceedings, LHC Lumi Days 2019: Prévessin, France, June 4–5, 2019*. 2019.

[23] CMS Collaboration, "The CMS trigger system", *JINST* **12** (2017) P01020, doi:10.1088/1748-0221/12/01/P01020, arXiv:1609.02366.

[24] W. Kozanecki, T. Pieloni, and J. Wenninger, "Observation of beam-beam deflections with LHC orbit data", CERN Accelerator Note CERN-ACC-NOTE-2013-0006, 2013.

[25] A. A. Babaev, "Coherent deflection of elliptic bunches colliding at crossing angle", 2021. arXiv:2104.02595.

[26] V. Balagura, "Van der Meer scan luminosity measurement and beam-beam correction", *Eur. Phys. J. C* **81** (2021) 26, doi:10.1140/epjc/s10052-021-08837-y, arXiv:2012.07752.

[27] A. Babaev et al., "Impact of beam-beam effects on absolute luminosity calibrations at the CERN Large Hadron Collider", 2021. To be submitted to *Phys. Rev. ST Accel. Beams*.

[28] M. Klute, C. Medlock, and J. Salfeld-Nebgen, "Beam imaging and luminosity calibration", *JINST* **12** (2017) P03018, doi:10.1088/1748-0221/12/03/P03018, arXiv:1603.03566.

[29] J. Knolle, "Measuring luminosity and the $t\bar{t}Z$ production cross section with the CMS experiment". PhD thesis, Universität Hamburg, 2020. CERN-THESIS-2020-185, DESY-THESIS-2020-020. doi:10.3204/PUBDB-2020-03187.